Karlsruhe Institute of Technology

Physics Laboratory
Laser Spectroscopy of Rubidium

Date of experiment

12.12.2018

	Name	Matrikel No.
1	Furkan Sahin	2259081
2	Adrian Dittmaier	2262233

Supervisor: Philip Schneider

Index

List of figures

1. Introduction

This report refers to the laboratory "Laser Spectroscopy of Rubidium". The goal of the lab is to resolute the hyperfine structure of the Rubidium atom, with the method of laser spectroscopy. In the following; all needed theory, the methods as well as the results of the experiments are given. Finally, the generated data are interrelated.

Laser spectroscopy is one category of the bright field of Spectroscopy[1]. One main application of spectroscopy is to identify and visualize the structure of atoms as well as molecules in an experimental environment. This is done by analysing the spectral lines of the investigated material. The outcome of this experiments allows us to make statements about material composition, physical- and chemical behaviour. Especially in material science laser spectroscopy is a frequently used method.

---

[1] Study of the interaction between matter and electromagnetic radiation.

2. Theory

In this section, the theory needed to perform the experiment is discussed.

a) Confocal Fabry Pérot Resonator

The Confocal Fabry Pérot Resonator is, as the name implies, a resonator with spherical mirrors. The mirrors have the same curvature of $R = 2f$ and are positioned at distance $l = 2f$. Light coupled into the resonator is reflected from the mirrors infinite times. Due to interference effects, only electromagnetic waves matching the standing wave condition are stable in the resonator.

$$\lambda_m = \frac{4l}{m} \qquad m \in \mathbb{N} \tag{1}$$

By substituting the resonance wavelength λ_m with the resonance frequency ν_m divided by the speed of light, one gets the following

$$\nu_m = \frac{c}{4l} m \qquad m \in \mathbb{N} \tag{2}$$

This frequency fulfilling condition (2) results in the eigenmodes of the resonator. The free spectral range (FSR) specifies the energetic distance between two modes with

$$FSR = \nu_m - \nu_{m-1} = \frac{c}{4l} \tag{3}$$

Further, a resonator´s quality is quantified by its Finesse. The Finesse is only evaluated by the losses within the resonator, these are related to the reflectivity *R* of the mirrors.

$$F = \frac{FSR}{\Delta\nu} = \frac{\pi R}{1 - R^2} \tag{4}$$

$\Delta\nu$ is the spectral linewidth of the resonator. By equation (3) and (2) it is observed that a longer resonator leads to a higher spectral width.

b) Spectral Lines

The penetration of an atom´s electron from a lower energetic level E_1 to a higher one E_2 can only be done in discrete values. In terms of photon absorption, this means only specific wavelengths are absorbed or emitted by the atom, the spectral lines. The corresponding resonance frequency ν of the spectral lines can be determined with

$$E_2 - E_1 = h\nu \tag{5}$$

Where as h is the Planck-constant. This leads to the assumption, that spectral lines have no width. Indeed, a certain range of wavelengths can fulfil the resonance condition of (5). This effect is called broadening. The reasons for the broadening are mentioned in the next section.

c) Broadening Effects

Already Heisenberg's uncertainty principle forbids infinitely sharp spectral lines, this broadening is called *natural linewidth*. The fact that every excited state has a finite lifetime τ shows that the corresponding energy level will have some width.

$$\Delta E \cdot \Delta t \geq \frac{\hbar}{2} \tag{5}$$

Hence the spectral lines show a certain width. Taking no further broadening effect in consideration, the profile of a transition frequency ω_0 is the one of a Lorentzian

$$\frac{I(\omega)}{I_0} = \frac{\gamma \,/\, 2\pi}{(\omega - \omega_0)^2 + (\gamma \,/\, 2)^2} \tag{6}$$

Where I_0 is the maximum intensity and the full width half maximum is $\gamma = \frac{1}{\tau}$.

Another broadening effect which has to considered, is the *Doppler broadening*. As the name implies this broadening refers to the Doppler effect. The velocity v_z of particles, which refers to the thermal energy of the probe, in the propagation direction of light causes a shift in the resonance frequency ω_0. This Shift can be determined by.

$$\bar{\omega}' = \bar{\omega}_0 \left(1 - \frac{v_z}{c}\right) \tag{7}$$

Doppler broadening is approximately 2 orders of magnitude bigger than the natural broadening. In case of the Rubidium atom at room temperature, the Doppler effect leads to a broadening of approx. 1 GHz. Hyperfine structure of Rubidium atom can not be resolved under this circumstance with absorption spectroscopy.
Under the assumption that other broadening effects are negligible, the Doppler broadening can be described by a Gaussian distribution.

$$I_{(\omega)} = I_0 \cdot e^{-\left(\frac{\omega - \omega_0}{\delta\omega \backslash \sqrt{4\ln(2)}}\right)^2} \tag{8}$$

Where the FWHM δ_w of the Gaussian profile is

$$\delta_\omega = \frac{\omega_0}{c} \sqrt{\frac{8 k_B T \ln(2)}{m}} \tag{9}$$

T is the Temperature of the object, *k*$_B$ is the Boltzmann-constant and *m* is the particle mass.

d) The Rubidium atom

The Rubidium atom belongs to the chemical group of alkali metals, hence it has single valence electron and is Hydrogen like. Natural Rubidium consists of 72.17% of stable ^{85}Rb and 27.83% of quasi-stable ^{87}Rb. Moreover; ^{83}Rb, ^{84}Rb and ^{86}Rb can be found, these isotopes are instable and therefore negligibly. The corresponding nuclear spins to the stable isotopes are I_{85Rb}=5/2 and I_{87Rb}=3/2.

e) Fine structure

For an adequate understanding of atomic structures relativistic corrections as well as the electron spin have to be taken into consideration. The fine structure comes from the coupling of a magnetic moment and magnetic field. The coupling occurs because of the electron spin s and the orbital movement of the electron l. These two can be described in a total angular momentum of the electron j.

$$j = s + l \tag{10}$$

With the electron spin $s = \pm\frac{1}{2}$, the energy levels for the fine structure split in two components $j = l \pm \frac{1}{2}$. Since the fine structure is just a matter of electron movement these one is the same for all isotopes of an atom. This additional energetic component in the atom structure is called *fine structure*.

f) Hyperfine structure

Taking the nucleus spin of the atom in to account, leads to an even higher splitting of spectral lines, the *hyperfine structure*. The angular momentum I of the nucleus and the total angular moment of the electron j end in a coupling analogous to the fine structure. These lead to the total angular momentum

$$F = j + I \tag{11}$$

The different nuclei for the ^{85}Rb and ^{87}Rb have a different nuclear spin and therefore a different hyperfine structure. An additional relative shift of the spectral lines, called *isotopic shift,* is related to physical properties like charge distribution in the nucleus, mass and volume

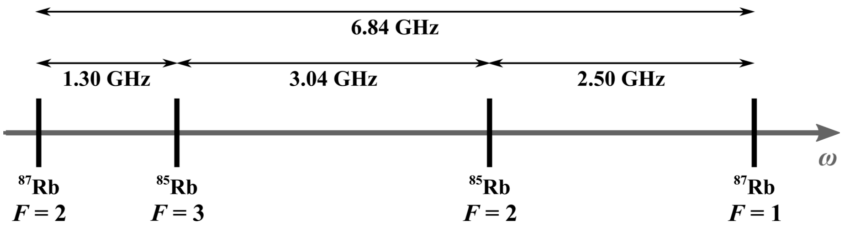

Figure 1 Isotopic shift of the $5^2s_{1/2}$ hyperfine splitting [1][2]

The overall structure for the D_1 line ($5^2s_{1/2} \leftrightarrow 5^2p_{1/2}$) and D_2 line ($5^2s_{1/2} \leftrightarrow 5^2p_{3/2}$) of Rubidium 85 and 87 is shown in picture. The experiment is focused on the D_2 line.

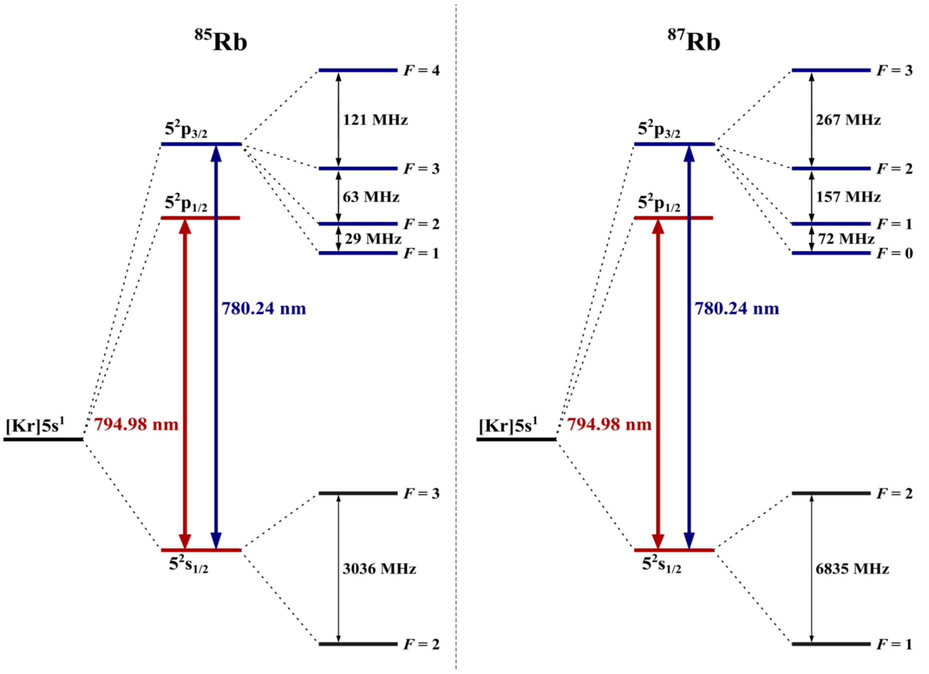

Figure 2 Fine- and hyperfine splitting of ^{85}Rb and ^{87}Rb. D_1 transition marked red, D_2 transition marked blue [1][2].

All transitions between two energy levels emerge in the total spectrum of Rubidium. A bunch of selection rules define which transitions an electron can do. The selection rules are based on atomic quantities $\Delta s, \Delta l, \Delta j$ and ΔF.

3. Experimental Setup

In this section all setups concerning the experiments are described. The D_2 transition is measured with the absorption- and saturation spectroscopy. The D_1 transition is not observable with the used laser light source.

a) Determining The Lasing Threshold

The goal of the first experiment is to determine the lasing threshold for the used semiconductor laser. To do so, the setup described below (see *figure 3*) is used.

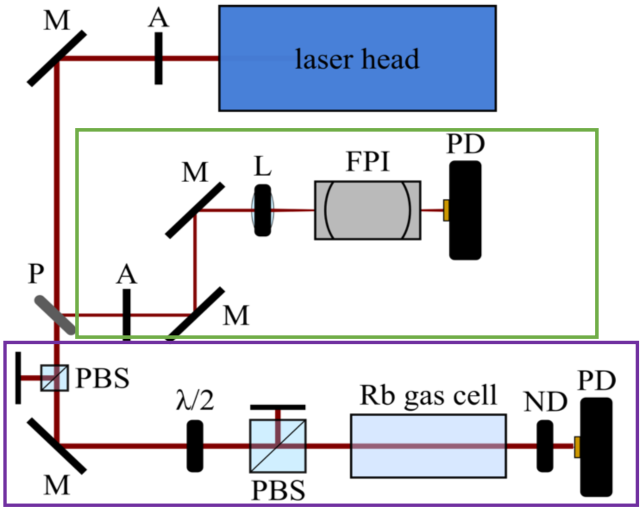

Figure 3 Schematic principle of the experimental set up for absorption spectroscopy

The outcoupled laser beam is goes through aperture A, the aperture is just for handling issues in order to stop the beam easily if necessary. Afterwards the beam is reflected from a mirror M towards a platelet P, which reflects a small amount of the laser beam by 90°.
The determining of the lasing threshold happens in the path of the 90° reflected beam (see *figure 3*, marked by green rectangular). After passing a second aperture, the beam is reflected from to mirrors. The lens L focuses the beam before it is induced in the Fabry-Pérot resonator and afterwards transmitted on to a photodiode P.
The Fabry-Pérot resonator is needed later in order to a have a reference for the rubidium transmissions. With the FSR it is then possible to calculate (3) the differences in frequencies.

To determine the lasing threshold the injection current of the diode laser is increased stepwise.

b) Absorption Spectroscopy

For this measurement the beam which surpasses the platelet (see *figure 3*, marked with violet rectangular) is considered. The polarizing beam splitter PBS reflects all light that is not polarized in the orientation of the PBS.
After the PBS the beam is considered as linear polarised. The combination of the retarder plate λ/2 and the PBS afterwards work is an adjustable intensity filter. Depending on the orientation

of the retarder plate, which changes the orientation of polarization, the PBS will then reflect more or less light.
The Rb gas cell contains the Rubidium atoms at a pressure of $1 \cdot 10^{-8}$ Torr and a volume of 35.2 ml. After the gas cell the beam passes a neutral density filter ND and afterwards a photodiode.

For the absorption spectroscopy the diode laser is tuned with the Littrow configuration. This enables to keep the laser beam in range of λ=778.99nm-788.40nm with a hope-free tuning range of maximum 23 GHz.
When the laser beam matches the frequency of the D_2 transition the photons become absorbed by the Rb. This is seen as an intensity at the photodiode.
The maximal resolution of this setup is, due to the Doppler broadening, 1GHz. This is higher than the hyperfine structure consequently only the fine structure is observable.

c) Saturation Spectroscopy

The goal of the saturation spectroscopy is to resolve the hyperfine structure. For this experiment two laser beams of same wavelength are needed: a stronger pump beam (1-p) and a weaker antiparallel probe beam (p≈0.05 of total intensity). Only the probe beam is to be detected by the photo diode.
As the two beams propagate in opposite direction each beam is absorbed equally by Rb atoms with velocity $|v_z|$, hence the recorded intensity is the same as the absorption spectroscopy one.
In case the laser wavelength is resonant with a transition $\lambda = \lambda_0$, both beams are absorbed by particles of velocity v_z=0. Since the high intensity pump beam have already depopulated the majority of the atoms (saturation), the probe beam will face less absorptions. This is seen as a slight intensity increase called *Lamp-dip*. Only atoms with velocity v_z=0 causes Lamb dips therefore these are Doppler-free, which enables to see the hyperfine structure.

Crossover Peaks

The recorded spectrum of D_2 shows more dips than allowed transitions. The wavelength λ of the laser beam in between two transitions λ_1 and λ_2, additional dips can occur due to the Doppler effect of atoms moving with velocity v. Since the movement of gases contributes to the Boltzmann-distribution it is more likely to find atoms moving with velocity ±v than v_z=0, therefore the crossover peaks show a higher intensity.

For this measurement the experimental setup hast be changed (see *figure 4*).

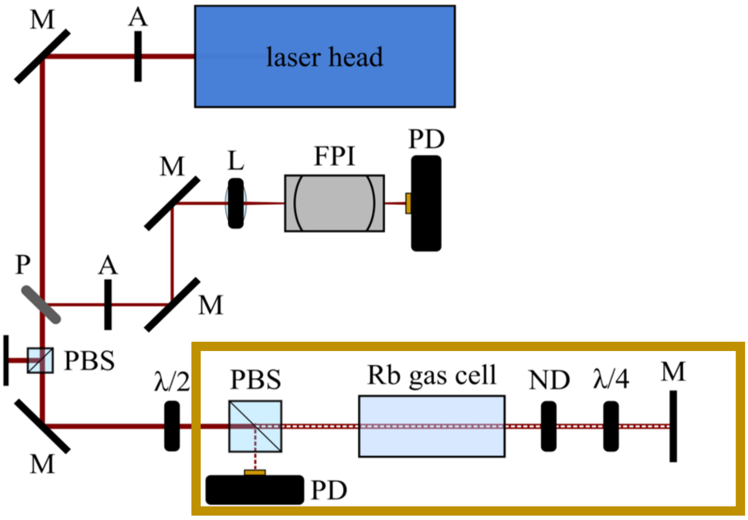

Figure 4 Schematic principle of the experimental set up for saturation spectroscopy

The following explanation contributes only to the change in the experimental setup (see *figure 4,* marked with gold rectangular). As the laser beam passes the PBS it enters the gas cell with full intensity (pump beam). After the gas cell the beam will pass a ND, a retarder plate λ/4, is reflected from the mirror (phase jump of polarisation of 180°), the retarder plate λ/4 (again) and finally a second time through the ND. This leads to an antiparallel beam with less intensity (probe beam), which has a polarization 90° to the original one (pump beam). After passing the Rb gas cell the probe beam is reflected, due to its polarization, at the PBS by 90°. The reflected probe beam then enters the photodiode.

4. Results

In this section the results of the experiments are presented and explained. The interpretation is done in the las section *5. Conclusion.*

a) Lasing threshold

In the first experiment the lasing threshold for the diode laser is to be determined. In the graph (see *figure 5)* the output voltage of the photo diode is plotted over the injection current of the diode laser.

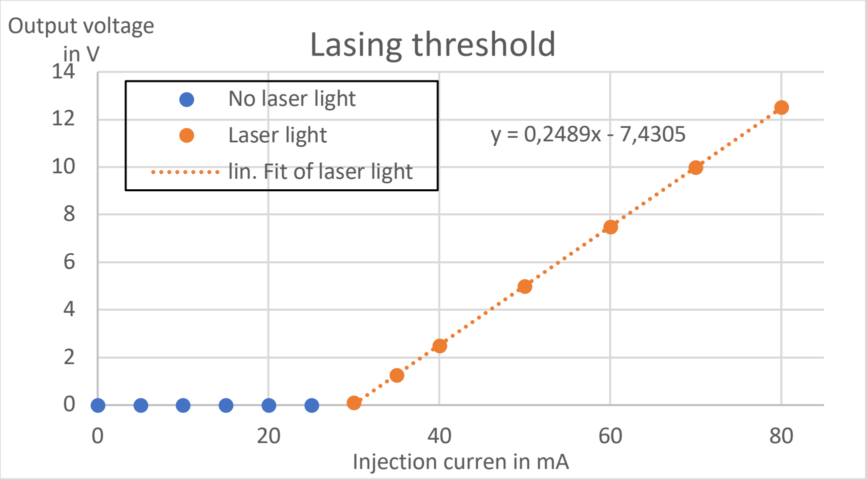

Figure 5 Determining of lasing threshold

Before the lasing condition is reached the output of the photodiode is equal zero. However, in the range from 0 mA to 25 mA a slight increase in the mV range is observed. The reason for this is that a higher injection will lead to more spontaneous emission, what is detected.

By fitting the measuring points at which the laser occurs the lasing threshold is determined. With the performed experiment the lasing threshold is at **29.85 mA**.
The output measurement took place with automatic calculation function of the oscilloscope, therefore the provided data are trustworthy. Uncertainties could refer to the injection current, unfortunately the manual does not provide information about the accuracy of the used power supply.

b) FPI Calibration Curve

With the FPI it is possible to translate the time distances of the resonator modes into frequency distances. This is an indirect calibration of the system. A direct way would be the calibration with a spectrometer.
Since many modes are in the FPI, the calculation is done for just four of them. A more accurate way would be to do it for all modes in the resonator.
Each mode is fitted with a Lorentzian, then the distances between the high points of each fit is calculated. These are the time distance between the modes.

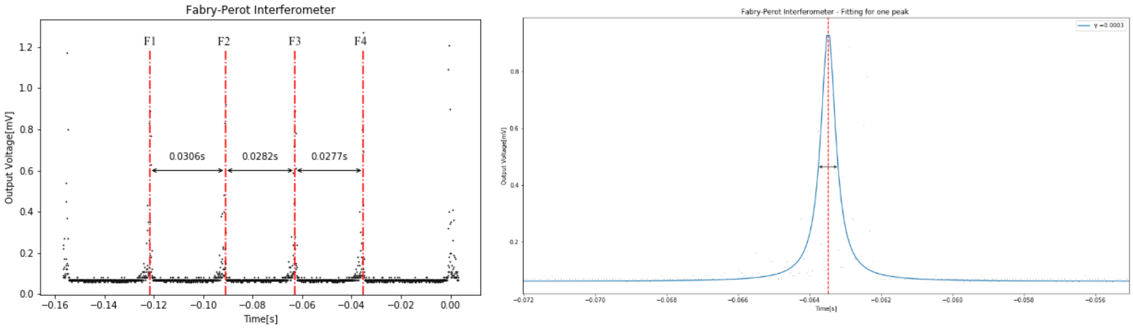

Figure 6 Calibration of FPI with corresponding fit of a mode

The distance between two modes **0,029±0,0015 s**.
The Free Spectral Range can be calculated (3) by given resonator length of 29±0.2 mm and the resonator in air (refractive index n≈1). The FSR is **2.59±0.02 GHz**. Hence, the frequency range within 1s is equal to **89±5 GHz**

c) Finesse

To determine the finesse experimentally, the peak width-full at half maximum (FWHM) Δv of the resonator modes and the FSR are needed (4). FSR is already defined in the previous section and Δv can be found by analysing the Lorentzian fits of the resonator modes **($\boldsymbol{\Delta v = 22 \pm 1.3}$ MHz)**.

$$F_{mess} = \frac{FSR}{\Delta v} = 1177 \pm 7.6$$

In addition, the theoretical finesse can be calculated with the given reflectivity of 99.85±0.05 % for the FPI.

$$F_{theo} = \frac{\pi \cdot \sqrt{R}}{1 - R} = 2100 \pm 700$$

The high uncertainty in F_{theo} refers to the denominator, which becomes very sensitive to small changes as R is close to one.
F_{mess} and F_{theo} do not match each other pretty well. The relative error is in the range of 15,4 % to 58,2 %. The inadequate deviation of theoretical and measured value could refer to Δv.
An insufficient amount of data points concerning the Lorentzian fit of the modes might lead to a slightly wrong FWHM, the same counts for the FSR which is also fit based. Also a in sufficient calibration of the FPI could lead to such an deviation.

d) Absorption Spectroscopy

After deducing the triangle signal occurring from the continuous frequency change, the intensity drops in the waveform can be fitted by Gaussian (see *figure 7)*. For easier evaluation the final wave form is inverted so the peak shows in positive direction.

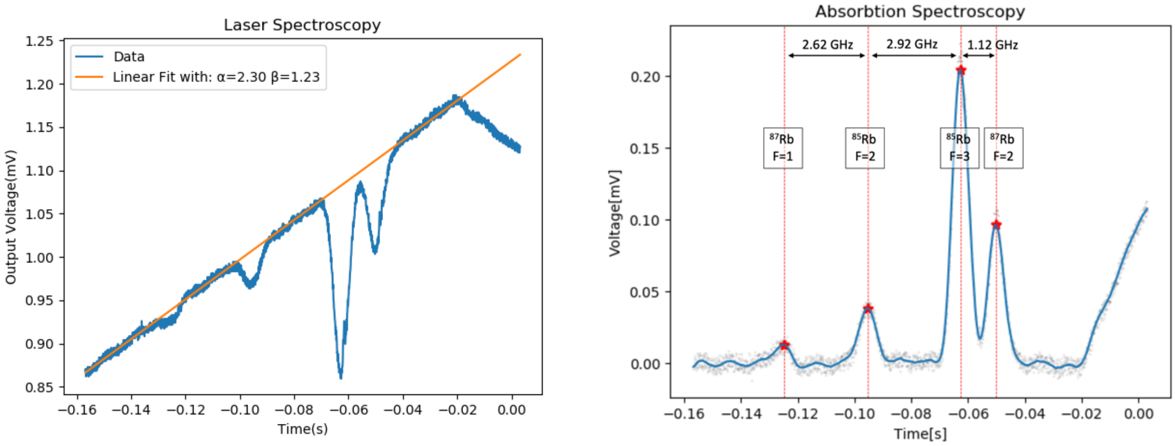

Figure 7 Absorption spectroscopy: Pure measured data (left), fitted and analysed waveform (right).

With the calibration of the FPI and the time distances between the peaks it is possible to determine the frequency distances between the peaks. By Knowing the expected fine structure of the Rb atom, it is possible to name each transition.

The uncertainty for the calculation refers to the uncertainty in the frequency (see *4 b) FPI calibration curve).* Other uncertainties, like statistical error in the data analyses, especially for the fits, are difficult to quantify and therefore not considered.

The transition of ^{85}Rb is determined with 2.92±0.16 GHzThe the one of ^{87}Rb is measured with 6.66±0.37. While the ^{87}Rb does match the theoretical value pretty good, the ^{85}Rb is a bit too low. Yet, including the uncertainty the measured transition contributes still do literature (see *figure 1*).

e) Doppler Broadening

In this section a closer look on the Doppler broadening is taken. For this the ^{85}Rb F=2 level is investigated further (see *figure 8)*. Since the Doppler broadening refers to the temperature, the given data allows to calculate (10) temperature in the gas cell. For easier evaluation the wave form is inverted so the peak shows in positive direction.

With the conducted fit the FWHM can be determined, the measured FWHM[2] is **340±20 MHz**. v_0 is the transition of D_2 with 780.24 nm and the mass of ^{85}Rb m=84.91 u.

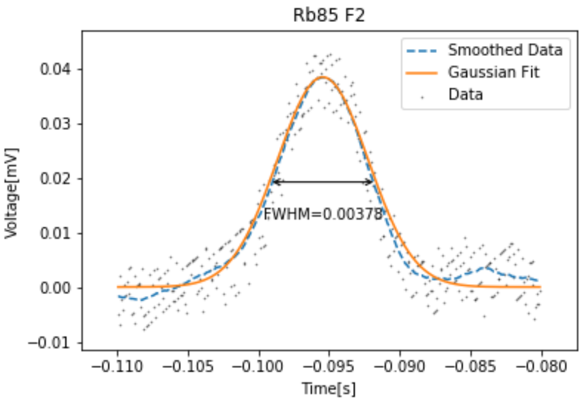

Figure 8 Doppler broadening of ^{85}RB F2

---

[2] FWHM for Gaussian = $2 \cdot \sqrt{2 \cdot \ln(2)} \cdot standard\ deviation$

The calculated temperature is equal to **130±15 k** (-143±15 °C). This is by far too cold, the ambient temperature in the room was 20 °C therefore the gas should have a similar temperature.

The most suitable explanation is that the Gaussian fit is not trustworthy. The FWHM for a reliable calculation of the temperature is about 510 MHz (50 % higher than measured). Also an insufficient calibration of the FPI could lead to such an deviation.

f) Saturation Spectroscopy

In the last experiment the goal is to resolute the hyperfine structure with the saturation spectroscopy, explained in section *3 c) saturation spectroscopy.* All parameters concerning the operation of the laser stay the same as for the absorption spectroscopy.

The Lamp-dips can be found now in the spectrum of the Doppler broadening. The dips have nearly solely the natural broadening and are therefore fitted by Lorentzian.

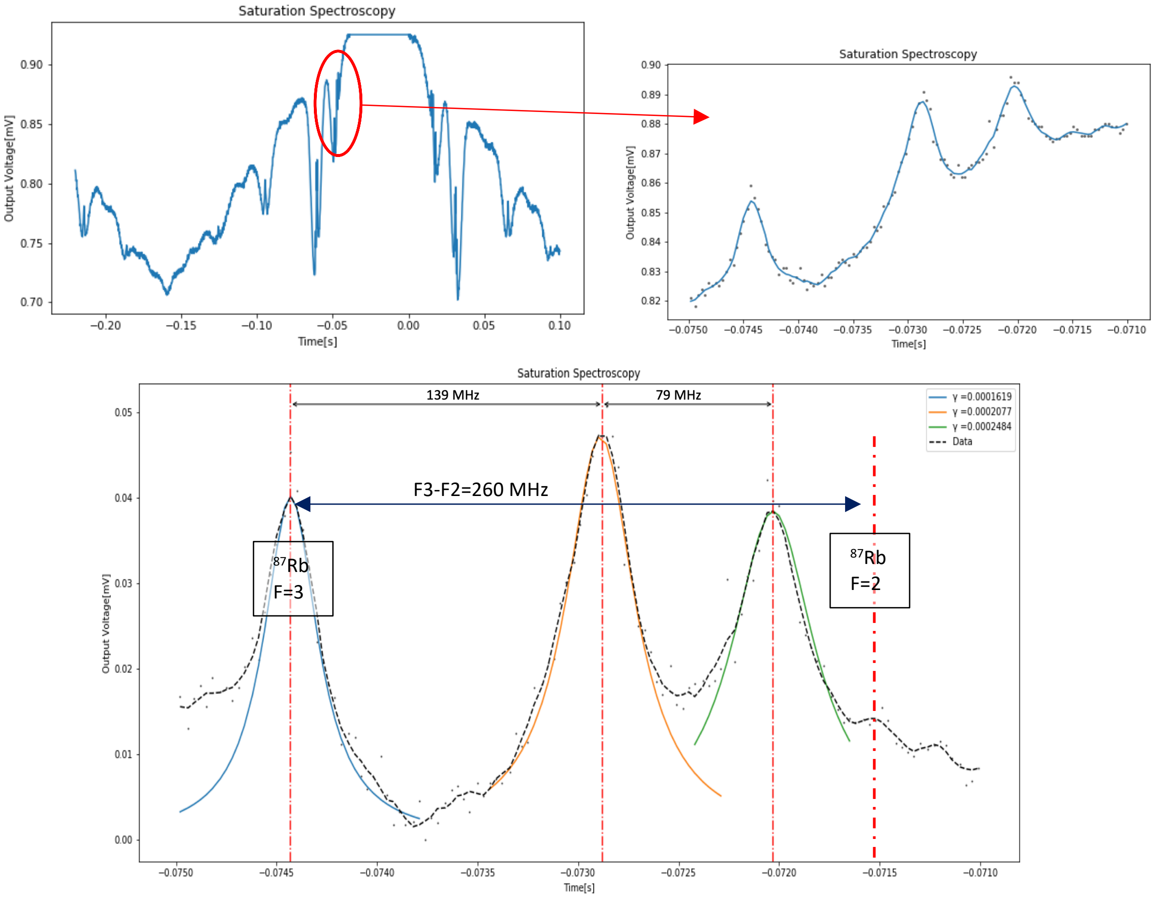

Figure 9 Lamp dibs in the Doppler spectrum of the ^{87}Rb

The gathered data are not sufficient for the ^{85}Rb therefore just do transition of ^{87}Rb is further analysed.

The frequency distances between the peaks are 139±8 MHz and 79±4 MHz. Unfortunately, these transitions do not refer to literature, therefor the orange and the green fit seem to be cross over peaks.

Indeed, there seem to be one of the hyperfine splitting transitions observable. the F2-F3 frequency difference measured with 260±14 MHz. However, the intensity peak of the

^{87}Rb F=2 is very low and the poor data source do not even allow a proper fit. Additionally the noise of the signal also leads to high points within the waveform.
The F2-F3 transition can just be found by knowing the energy distances of the hyperfine structure. Although sketched in the graph (see *figure 9*), the provided measurement should not be considered as an experimental prove.

5. Conclusion

The in the lab “Laser Spectroscopy” give an insight in to the huge field of Spectroscopy. The executed experiments show how the structure of atoms can be measured and what difficulties can occur.
The Rubidium atom was observed with the absorption- and saturation spectroscopy. The fine structure of the atom could resolute properly, the calculated transitions are also close to the theoretical ones. The hyperfine structure could not be resolved in a sufficient way. The signal noise and lack of data points lead to this unsatisfactory result.

To improve the result of future experiments especially the calibration of the FPI should be enhanced. The lack of data point due to zero intensity in between the resonator modes makes the calibration too uncertain.

6. Reference

[1] Marcel Schrodin: Laser Spectroscopy Lab (2018), Karlsruhe Institute of Technology provided lab manual

[2] Daniel A. Steck, *Rubidium 85 D line data, Rubidium 87 D line data,* 2008 available online *at* http://steck. us/alkalidata

[3] Gerd Litfin, *Technische Optik in der Praxis*, Springer-Verlag Berlin Heidelberg, 2013